

Communication: *Ab initio* simulations of hydrogen-bonded ferroelectrics: Collective tunneling and the origin of geometrical isotope effects

K. T. Wikfeldt^{1,a)} and A. Michaelides²

¹Science Institute, University of Iceland, Nordita, Stockholm, Sweden and University College London, London WC1E 6BT, United Kingdom

²Thomas Young Centre, London Centre for Nanotechnology and Department of Chemistry, University College London, London WC1E 6BT, United Kingdom

(Received 22 November 2013; accepted 7 January 2014; published online 22 January 2014)

Ab initio simulations that account for nuclear quantum effects have been used to examine the order-disorder transition in squaric acid, a prototypical H-bonded antiferroelectric crystal. Our simulations reproduce the >100 K difference in transition temperature observed upon deuteration as well as the strong geometrical isotope effect observed on intermolecular separations within the crystal. We find that collective transfer of protons along the H-bonding chains – facilitated by quantum mechanical tunneling – is critical to the order-disorder transition and the geometrical isotope effect. This sheds light on the origin of isotope effects and the importance of tunneling in squaric acid which likely extends to other H-bonded ferroelectrics. © 2014 Author(s). All article content, except where otherwise noted, is licensed under a Creative Commons Attribution 3.0 Unported License. [<http://dx.doi.org/10.1063/1.4862740>]

Ferroelectric materials have been extensively examined because of their many diverse applications in, *e.g.*, electro-optic, piezoelectric, and random access memory devices.¹ Recently, interest has intensified in hydrogen (H-) bonded ferroelectrics because of the discovery of above room-temperature ferroelectricity in an organic crystal and the realization that they could potentially be used as cheaper and more environment friendly organic electronics.^{2–4} H-bonded ferroelectrics are also a valuable class of materials through which we can gain deeper understanding of the fundamental nature of H-bonding. Primarily this is because they are well-characterized crystalline materials with a range of H-bonding configurations and in most cases have been synthesized in both their standard and deuterated forms.

Many H-bonded ferroelectrics exhibit phase transitions to paraelectric (PE) phases that lack long-range ordering of protons in the H-bonds. The Curie temperature (T_c) of these transitions can dramatically increase by ~ 100 K upon deuteration but the physical origin of this effect is still not fully understood. An early model^{5,6} explained this giant isotope effect on the basis of tunneling of protons in double well potentials. However, this model fails to account for experimentally observed geometrical isotope effects in H-bonding geometry between the protonated and deuterated crystals, where H-bonds have been observed to elongate upon deuteration^{7,8}—a so-called Ubbelohde effect.^{9,10} Models involving a coupling between lattice modes and proton dynamics were therefore suggested.^{11,12} It was argued on these grounds that tunneling is unnecessary to explain the large increase of T_c upon deuteration.⁷ On the other hand, neutron Compton scattering experiments on the commonly studied KH_2PO_4 (KDP) system¹³ showed that protons occupy both sites along the H-bonds on a short time-scale above its phase transition

at 124 K, indicating coherent quantum tunneling, while no such coherence was found in the deuterated crystal.¹⁴ Theoretical work^{15,16} attempted to reconcile these differing interpretations by suggesting that a mechanism behind the Ubbelohde effect may itself be collective tunneling in clusters of atoms in the crystal. However, direct *ab initio* simulations aimed at elucidating the mechanisms behind the isotope shift of T_c and Ubbelohde effects are challenging due to the complex coupled dynamics involving multiple H/D atoms, and the role of tunneling has thus remained unclear. In this context, squaric acid ($\text{C}_4\text{H}_2\text{O}_4$ or H_2SQ) provides an ideal simple model system which has been explored extensively by both experiments^{8,12,17–19} and theory.^{20–24}

Here we report results from large-scale *ab initio* path-integral molecular dynamics (PIMD) simulations of H_2SQ and its deuterated analogue D_2SQ that have allowed us to extract detailed information on quantum effects and collective proton behavior. *Ab initio* PIMD was recently applied to KDP,²⁵ but due to the limited system size where collective effects were neglected only the disordered paraelectric phase could be studied. We find that collective effects are vital for capturing antiferroelectric (AFE) order in the simulations. Further, the Ubbelohde effect is well reproduced by PIMD and the transition to paraelectric ordering occurs at higher temperature for D_2SQ compared to H_2SQ , in agreement with the experimental shift from $T_c(\text{H}_2\text{SQ}) = 373$ K to $T_c(\text{D}_2\text{SQ}) = 520$ K. Our simulations also reveal that tunneling is an important mechanism behind both the Ubbelohde effect and the collective proton jumps in the paraelectric phase.

Squaric acid is composed of planar $\text{C}_4\text{H}_2\text{O}_4$ molecules bound by strong H-bonds in 2D sheets with two slightly inequivalent H-bonding chains running along the *a*- and *c*-axes (see Fig. 1). The sheets in turn are stacked along the *b*-axis and weakly bound by dispersion forces. In the low-temperature antiferroelectric phase each layer is polarized due

^{a)}wikfeldt@hi.is

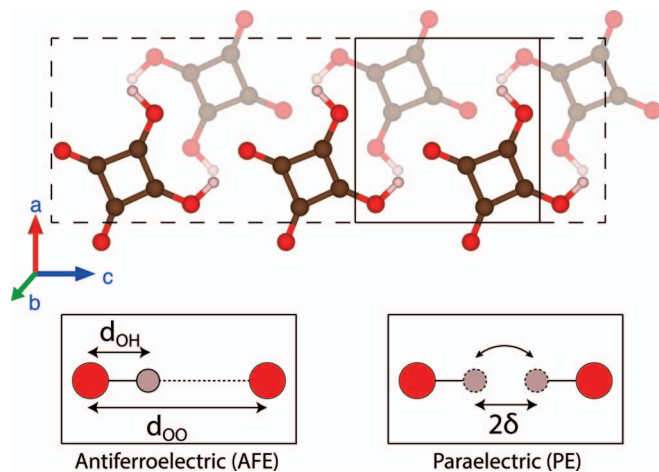


FIG. 1. Crystal structure of squaric acid. The solid and dashed squares in the upper panel denote the primitive unit cell and the $1 \times 1 \times 3$ supercell used for PIMD simulations, respectively. The lower panel illustrates the d_{OO} and δ structural parameters and the difference between AFE and PE ordering.

to long-range ordering of H atoms into equivalent sites in the H-bonds, with opposite polarization in neighboring planes, while in the high-temperature paraelectric phase the long-range ordering is lost due to proton disorder.

Realistic simulations of H-bonded ferroelectrics are challenging for several reasons. First, an accurate theoretical approach is needed that describes the H-bonds between the molecules, the proton transfer barriers and, in many cases, weak van der Waals bonding between molecules or layers of the material. Second, to capture the collective nature of proton ordering in squaric acid it is essential to use extended simulation cells with several molecular units along the H-bonding directions. Third, thermal and nuclear quantum effects such as tunneling and zero point motion must be taken into account given the finite temperature phase transition and the quantum mechanical nature of the proton. In tackling this system we considered all of these issues in detail. A more complete description of the theoretical approach employed and tests performed to establish its accuracy is given in the supplementary material.²⁶ In brief, the essential features of the simulations performed are that we used density functional theory (DFT) with projector-augmented wave (PAW) potentials²⁷ as implemented in the VASP code.^{28,29} Nuclear quantum effects were accounted for with PIMD (see, *e.g.*, Refs. 30 and 31 as implemented in VASP by Alfè and Gillan³²). Thirty-two path integral beads were used except for H₂SQ at 100-200 K where 64 beads were required and for D₂SQ at 300-500 K where 16 beads gave sufficiently converged quantum effects.²⁶ To capture collective effects we used $1 \times 1 \times 3$ supercells (Fig. 1) with a H-bonding chain of 3 molecular units along the *c*-axis and a total of 6 molecules in the cell. This setup also allowed us to investigate the role of collective effects by comparing the proton ordering along the *a*- and *c*-axes, which have been shown to be very weakly coupled.^{33,34} All simulations were performed in the canonical (NVT) ensemble with experimental lattice constants.²⁶ The vdW-DF2^{35,36} exchange-correlation (xc) functional was selected after an extensive series of tests showed that of the xc functionals considered it gave good agreement with experiment in terms of

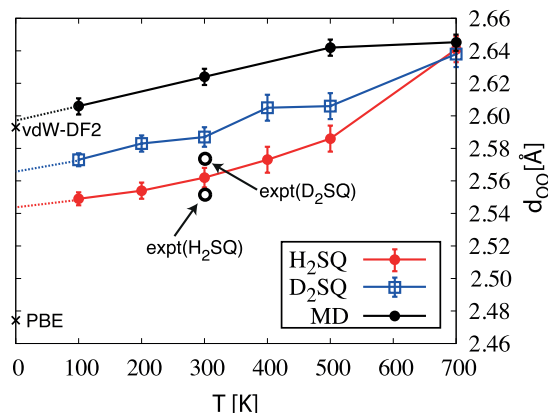


FIG. 2. Average oxygen-oxygen distances d_{OO} as a function of temperature for MD and PIMD simulations using vdW-DF2. d_{OO} values for optimized geometries using PBE and vdW-DF2 are shown by crosses at $T=0$. Experimental values for H₂SQ from Ref. 37 and D₂SQ from Ref. 8 at 300 K are marked by empty circles.

O-O intermolecular distances in PIMD simulations and produced a proton transfer barrier in closest agreement with results from explicitly correlated calculations. Specifically, while the commonly used Perdew-Burke-Ernzerhof (PBE) functional gives a proton transfer barrier of 18 meV, the vdW-DF2 gives 87 meV which is considerably closer to values from Møller-Plesset second order perturbation theory (MP2, 110 meV) and random phase approximation (RPA, 148 meV) calculations.²⁶

We begin by discussing oxygen-oxygen distances, d_{OO} , and their temperature and isotope dependence. Optimized d_{OO} values are shown by crosses in Fig. 2 where it can be seen that vdW-DF2 predicts a value higher than experiment. Moreover, MD simulations give average d_{OO} values that increase with temperature, extrapolating down to the optimized value at 0 K and severely overestimating d_{OO} for H₂SQ by 0.07 Å at 300 K compared to the experimental value. This thermal expansion is however completely counteracted by quantum effects in PIMD, where at 300 K the combined thermal and quantum effects reduce d_{OO} by 0.06 Å for H₂SQ and 0.04 Å for D₂SQ compared to the optimized value, resulting in agreement within 0.01 Å with the corresponding experimental values.^{8,37} The large discrepancy between optimized and PIMD values for d_{OO} shows that geometry optimizations can be in serious error in systems with strong H-bonds and that quantum effects must be accounted for. Note that the optimized PBE value severely underestimates the experimental d_{OO} , an error that is further exasperated by the inclusion of quantum effects, highlighting the failure of the common PBE approximation to describe squaric acid. The observed Ubbelohde effect in PIMD, *i.e.*, the difference in d_{OO} between H₂SQ and D₂SQ of around 0.02 Å as seen in Fig. 2, is in good agreement with experiments. Starting at around 500 K this isotope effect decreases and only around 700 K (above the decomposition temperature of H₂SQ³⁸) do the simulations predict the same d_{OO} . MD also gives the same d_{OO} as the PIMD simulations at 700 K, consistent with vanishing influence of quantum effects at high temperatures.

The d_{OO} values from MD and PIMD shown in Fig. 2 are calculated along the *c*-axis where the coupling between

three molecules is explicitly included. Interestingly, d_{OO} values along the a -axis where this coupling is neglected are shorter by around 0.02 \AA for both H_2SQ and D_2SQ . This shortening is connected to more frequent jumps of H and D atoms along the a -axis compared to the c -axis. Collective effects thus enhance the localization of H and D atoms resulting in longer H-bonds.

Seeing that the Ubbelohde effect is reproduced in PIMD we now examine the ordering behavior at different temperatures. The proton-ordered AFE phase in squaric acid is characterized by occupation of only one site in the H-bonds resulting in long-range order, while in the PE phase H/D jumps occur within clusters creating local defects and disrupting the long-range order. A convenient structural order parameter to quantify the ordering is the δ parameter, defined as $2\delta = d_{OO} - 2d_{OH}$ where d_{OH} is the intramolecular O-H (O-D) distance projected onto the OO axis (see Fig. 1, lower panel). Figures 3(a) and 3(b) reveal characteristics of both AFE and PE ordering in probability distributions $P(\delta)$ calculated from PIMD and MD simulations; a unimodal distribution reflects the absence of jumps while bimodality shows the presence of jumps. PIMD simulations of H_2SQ are ordered at 100 K but disordered at 200 K and above, while D_2SQ is ordered at 100-300 K but disordered at 400-500 K, in qualitative agreement with the known difference of around 150 K in T_c for the protonated and deuterated crystals. On the other hand, the MD simulations are ordered at all temperatures, reflecting the large impact of quantum effects. The limited simulation time and system size possible for *ab initio* PIMD precludes definitive conclusions on AFE or PE ordering in the simulations at a given temperature. However, these two approximations can be expected to partially cancel in these rough estimates of T_c since limited simulation time might overestimate T_c and insufficiently converged correlations along H-bonding chains should underestimate T_c .²⁶ As before, the $P(\delta)$ distributions shown in Fig. 3 are calculated along the c -axis, since distributions along the a -axis (not shown) are bimodal at all temperatures, even in MD.

As seen in Figs. 3(a) and 3(b) H atoms are significantly more likely to populate the centric $\delta = 0$ position compared to D atoms. Larger probability density at $\delta = 0$ leads to stronger and shorter H-bonds and is the main mechanism behind the Ubbelohde effect, as evidenced also by the minimum energy path of proton transfer which involves a shortening of d_{OO} by around 0.15 \AA in the $\delta=0$ transition state compared to the initial state. We now examine why there is an enhanced prob-

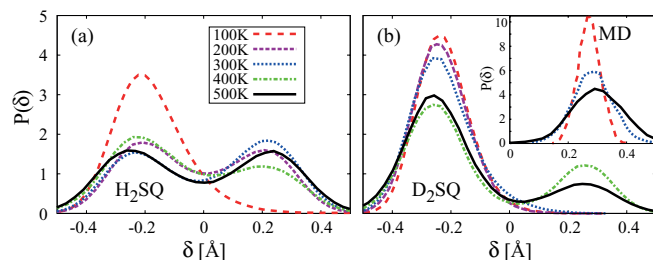


FIG. 3. Probability distributions of the δ parameter for (a) H_2SQ and (b) D_2SQ from PIMD, and (inset in (b)) from MD.

ability at $\delta = 0$ in the case of H compared to D atoms and in particular consider the role played by tunneling.

The role of tunneling is examined by considering the radius of gyration R_g of the H and D ring-polymers in our PIMD simulations. We calculate R_g for a single atom as $R_g^2 = \frac{1}{P} \sum_{i=1}^P (\mathbf{r}_i - \mathbf{r}_c)^2$ where the sum runs over the P beads and \mathbf{r}_c is the centroid position (center of the ring-polymer). R_g thus quantifies the delocalization of a quantum particle, which increases during tunneling. We find the average values $\langle R_g \rangle$ of H atoms to decrease from 0.19 \AA at 100 K to 0.14 \AA at 500 K, and correspondingly for D atoms to decrease from 0.15 \AA to 0.10 \AA . Next we extract the dependence of R_g on δ_c , *i.e.*, the δ parameter for the centroid coordinate, and furthermore decompose into components parallel (R_g^{\parallel}) and perpendicular (R_g^{\perp}) to the H-bonding vectors (see Fig. 4(c)). Figure 4(a) shows the behavior of $R_g^{\parallel}(\delta_c)$ and $R_g^{\perp}(\delta_c)$ for H_2SQ and D_2SQ along the c -axis. A clear temperature dependence is seen where, in particular, R_g^{\parallel} increases sharply for $\delta_c \rightarrow 0$ at lower temperatures for both H_2SQ and D_2SQ , indicating that tunneling contributes significantly when H/D atoms approach the centric position of the H-bonds. At higher temperature the increase in R_g^{\parallel} becomes smaller but not insignificant, indicating that tunneling takes place nearer to the top of the energy barrier due to thermal excitations. It can be seen that the R_g^{\parallel} curve for H_2SQ at 100 K extends to $\delta_c = 0$ with a sharp increase in the delocalization even though no collective jumps occur at this temperature (see Fig. 3), showing that protons can tunnel into the central barrier at low temperatures but quickly return to the original position due to the overall long-range order. In contrast, R_g^{\perp} is constant or decreases slightly as $\delta_c \rightarrow 0$. These results suggest that tunneling enhances the probability density of H atoms in the centric position and thus contributes directly to the Ubbelohde effect.

Tunneling also plays a direct role in collective proton jumps as shown in Fig. 4(b). For each of the 3 protons along the c -axis we compute the instantaneous values of δ_c and R_g^{\parallel} .³⁹ The upper panel of Fig. 4(b) shows several collective proton jumps during a selected portion of the simulation trajectory for H_2SQ at 200 K in one of the sheets and the lower panel shows the corresponding instantaneous delocalization. In the first shaded collective jump event the instantaneous R_g^{\parallel} of all protons is around the average and the jump thus appears to be mostly classical, *i.e.*, driven by thermal excitations. In the second event two protons show a large increase in R_g^{\parallel} and are clearly tunneling through a part of the energy barrier while the third proton appears to jump by thermal excitation, while in the last event all protons show an increase in delocalization. Similar combinations of tunneling and thermal excitations are seen at other temperatures and for D_2SQ , with the probability for non-tunneling thermal jumps increasing at higher temperatures (see additional figures in Ref. 26). To summarize, these results suggest that tunneling of several protons along an H-bonding chain not only contributes to the Ubbelohde effect but also, in combination with thermal fluctuations, plays a role in the disordering transition at T_c , above which the protons occupy both sites in the H-bonds with equal probability.

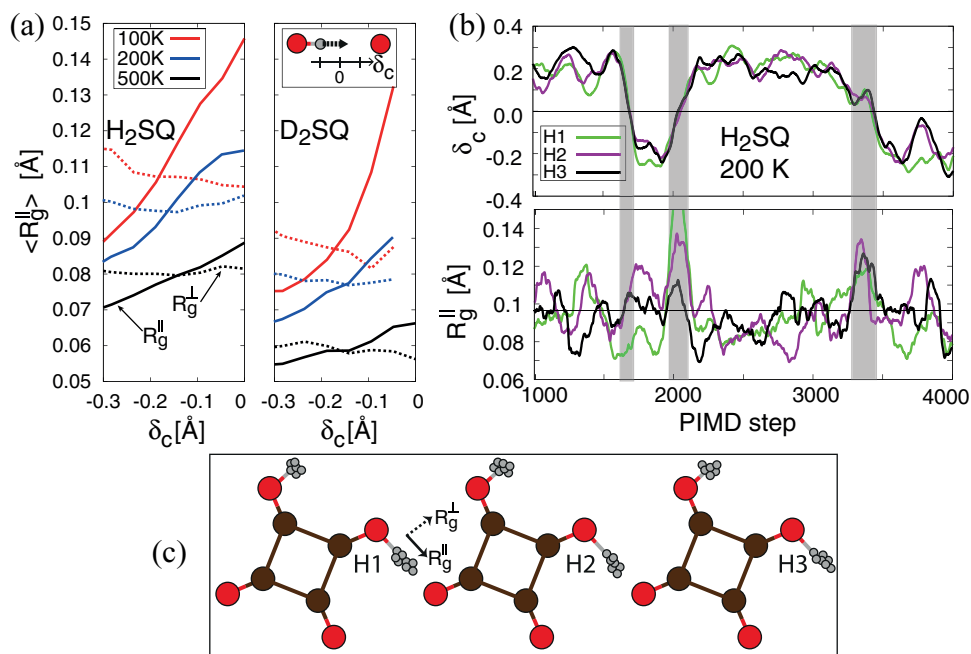


FIG. 4. (a) Radius of gyration of H/D ring polymers as a function of δ_c at different temperatures for H₂SQ (left) and D₂SQ (right). Parallel and perpendicular components of R_g are shown by solid and dashed lines, respectively. (b) Instantaneous H centroid positions (upper) and R_g^{\parallel} values (lower) for 3 protons along one H-bonding chain in H₂SQ at 200 K for a selected portion of the simulation trajectory. Shaded areas show collective proton jumps and the horizontal line in the lower panel indicates the average R_g^{\parallel} . (c) Schematic illustration of a collective proton jump and the delocalization of H ring-polymers.

In conclusion, we find that the combination of dispersion-including (vdW) DFT functionals and path-integral MD simulations can be used to realistically describe ordered and disordered phases of challenging H-bonded ferroelectrics such as squaric acid. A particularly important aspect of the simulations is the use of extended supercells that explicitly include correlations between H/D atoms along H-bonding chains. These correlations help to localize the H/D atoms and without their explicit treatment only disordered paraelectric behavior is found. Our PIMD simulations reveal pronounced nuclear quantum effects where the large quantum delocalization of H atoms and tunneling into the central barrier strengthen the H-bonds. The same effect is seen in the deuterated crystal but with smaller magnitude, leading to an Ubbelohde effect with an elongation of oxygen-oxygen distances by around 0.02 Å, in good agreement with experiment. The Ubbelohde effect in turn leads to a large shift in the temperature of the disordering AFE-PE transition upon isotopic substitution. Our simulations also suggest that concerted proton jumps in the disordered phase may take place through a combined effect of quantum tunneling of several protons combined with thermal fluctuations of nearby non-tunneling protons. These insights clarify the role played by tunneling in squaric acid but they are likely to extend to other H-bonded ferroelectrics, which calls for future simulation studies and experiments. The collective jump mechanism assisted by tunneling observed here may also contribute to proton transport in, *e.g.*, high pressure ice⁴⁰ and along water wires in biological environments⁴¹ and inside carbon nanotubes.⁴²

This research was partially supported by the European Research Council and made use of the HECToR super-

computer through membership of the UK's HPC Materials Chemistry Consortium which is funded by the Engineering and Physical Sciences Research Council (UK) (EPSRC) (EP/F067496). Computer time from the UK Car-Parrinello Consortium (UKCP) as well as the Abisko supercomputer through the Swedish National Infrastructure for Computing (SNIC) is also gratefully acknowledged. A.M. is also supported by the Royal Society through a Royal Society Wolfson Research Merit Award, and K.T.W. is supported by the Icelandic Research Fund through Grant No. 120044042.

- ¹R. Blinc, *Ferroelectrics* **267**, 3 (2002).
- ²S. Horiuchi, F. Ishii, R. Kumai, Y. Okimoto, H. Tachibana, N. Nagaosa, and Y. Tokura, *Nat. Mater.* **4**, 163 (2005).
- ³S. Horiuchi and Y. Tokura, *Nat. Mater.* **7**, 357 (2008).
- ⁴S. Horiuchi, Y. Tokunaga, G. Giovannetti, S. Picozzi, H. Itoh, R. Shimano, R. Kumai, and Y. Tokura, *Nature* **463**, 789 (2010).
- ⁵R. Blinc, *J. Phys. Chem. Solids* **13**, 204 (1960).
- ⁶R. Blinc and S. Svetina, *Phys. Rev.* **147**, 423 (1966).
- ⁷M. I. McMahon, R. J. Nelmes, W. F. Kuhs, R. Dorwarth, R. O. Piltz, and Z. Tun, *Nature* **348**, 317 (1990).
- ⁸M. I. McMahon, R. J. Nelmes, W. F. Kuhs, and D. Semmingsen, *Z. Kristallogr.* **195**, 231 (1991).
- ⁹A. R. Ubbelohde and K. J. Gallagher, *Acta Crystallogr.* **8**, 71 (1955).
- ¹⁰X. Z. Li, B. Walker, and A. Michaelides, *Proc. Natl. Acad. Sci. U.S.A.* **108**, 6369 (2011).
- ¹¹A. Bussmann-Holder and K. H. Michel, *Phys. Rev. Lett.* **80**, 2173 (1998).
- ¹²N. Dalal, A. Klymchyov, and A. Bussmann-Holder, *Phys. Rev. Lett.* **81**, 5924 (1998).
- ¹³G. F. Reiter, J. Mayers, and P. Platzman, *Phys. Rev. Lett.* **89**, 135505 (2002).
- ¹⁴G. Reiter, A. Shukla, P. Platzman, and J. Mayers, *New J. Phys.* **10**, 013016 (2008).
- ¹⁵S. Koval, J. Kohanoff, R. L. Migoni, and E. Tosatti, *Phys. Rev. Lett.* **89**, 187602 (2002).
- ¹⁶S. Koval, J. Kohanoff, J. Lasave, G. Colizzi, and R. L. Migoni, *Phys. Rev. B* **71**, 184102 (2005).

- ¹⁷J. Petersson, *Ferroelectrics* **35**, 57 (1981).
- ¹⁸A. Katrusiak and R. Nelmes, *J. Phys. C: Solid State Phys.* **19**, L765 (1986).
- ¹⁹D. Semmingsen, Z. Tun, R. J. Nelmes, R. K. McMullan, and T. F. Koetzle, *Z. Kristallogr.* **210**, 934 (1995).
- ²⁰S. Dolin, A. Levin, T. Y. Mikhailova, M. Solin, and N. Zinova, *Int. J. Quantum Chem.* **111**, 2671 (2011).
- ²¹C. Rovira, J. J. Novoa, and P. Ballone, *J. Chem. Phys.* **115**, 6406 (2001).
- ²²J. Palomar and N. S. Dalal, *Ferroelectrics* **272**, 173 (2002).
- ²³A. Bussmann-Holder and N. Dalal, *Structure and Bonding* (Springer, 2007), Vol. 124, pp. 1–21.
- ²⁴H. Ishizuka, Y. Motome, N. Furukawa, and S. Suzuki, *Phys. Rev. B* **84**, 064120 (2011).
- ²⁵V. Srinivasan and D. Sebastiani, *J. Phys. Chem. C* **115**, 12631 (2011).
- ²⁶See supplementary material at <http://dx.doi.org/10.1063/1.4862740> for computational convergence tests, comparisons between DFT functionals and MP2 and RPA calculations, and additional figures displaying collective proton jumps.
- ²⁷G. Kresse and D. Joubert, *Phys. Rev. B* **59**, 1758 (1999).
- ²⁸G. Kresse and J. Furthmüller, *J. Comput. Mater. Sci.* **6**, 15 (1996).
- ²⁹G. Kresse and J. Furthmüller, *Phys. Rev. B* **54**, 11169 (1996).
- ³⁰D. Marx and M. Parrinello, *Z. Phys. B* **95**, 143 (1994).
- ³¹M. E. Tuckerman, D. Marx, M. L. Klein, and M. Parrinello, *Science* **275**, 817 (1997).
- ³²D. Alfè and M. J. Gillan, *J. Chem. Phys.* **133**, 044103 (2010).
- ³³K.-D. Ehrhardt, U. Buchenau, E. Samuelsen, and H. Maier, *Phys. Rev. B* **29**, 996 (1984).
- ³⁴J. Palomar and N. Dalal, *J. Phys. Chem. B* **106**, 4799 (2002).
- ³⁵K. Lee, É. D. Murray, L. Kong, B. I. Lundqvist, and D. C. Langreth, *Phys. Rev. B* **82**, 081101 (2010).
- ³⁶J. Klimeš, D. R. Bowler, and A. Michaelides, *Phys. Rev. B* **83**, 195131 (2011).
- ³⁷D. Semmingsen, F. J. Hollander, and T. F. Koetzle, *J. Chem. Phys.* **66**, 4405 (1977).
- ³⁸K.-S. Lee, J. Jung Kweon, I.-H. Oh, and C. Eui Lee, *J. Phys. Chem. Solids* **73**, 890 (2012).
- ³⁹No dynamical information can be obtained from PIMD simulations but the trajectories sample the quantum mechanical configuration space and Fig. 4(b) thus demonstrates real correlations in the system.
- ⁴⁰E. Schwegler, M. Sharma, F. Gygi, and G. Galli, *Proc. Natl. Acad. Sci. U.S.A.* **105**, 14779 (2008).
- ⁴¹Z. Smedarchina, W. Siebrand, A. Fernández-Ramos, and Q. Cui, *J. Am. Chem. Soc.* **125**, 243 (2003).
- ⁴²J. Chen, X.-Z. Li, Q. Zhang, A. Michaelides, and E. Wang, *Phys. Chem. Chem. Phys.* **15**, 6344 (2013).